Color of postponed magnetic noise in $K_{0.4}[Cr(CN)_6][Mn(R/S)\text{-}pn](R/S)\text{-}pnH_{0.6}$ molecular ferrimagnet

R. B. Morgunov[1,2,*] and A. D. Talantsev[1]

[1]*Institute of Problems of Chemical Physics, Russian Academy of Sciences, Chernogolovka, 142432, Russia*

[2]*Tambov State Technical University, Tambov, 392000, Russia*

(Received 24 June 2016; revised manuscript received 2 September 2016; published 19 October 2016)

Exotic conditions for the existence and evolution of nonlinear spin ensembles (domain walls, spin solitons, skyrmions) in molecular-based magnets are incarnated in the macroscopic response of magnetization corresponding to collective stochastic behavior. The molecular ferrimagnet $K_{0.4}[Cr(CN)_6][Mn(R/S)\text{-}pn](R/S)\text{-}pnH_{0.6}$ manifests three types of magnetic relaxation: (a) continuous decay of magnetic moment, (b) stepwise relaxation by stochastic magnetization jumps, and (c) a single jump of magnetization in threshold magnetic field. Continuous relaxation at 20–50 K is provided by domain wall movement described in the frames of a strong pinning model, while a low-temperature continuous component of relaxation does not follow this model. Stepwise stochastic relaxation was observed below 8 K in both a sweeping reverse magnetic field and a stationary reverse magnetic field. Statistical treatment of the postponed magnetization jumps revealed a multimodal amplitude distribution of stochastic magnetization jumps corresponding to magnetic moment transitions between few clear distinguishable levels. Spectral density of magnetization jumps in a stationary magnetic field corresponds to white noise, while spectral density in a sweeping magnetic field manifests pink noise $\sim 1/f$ provided by self-organized criticality. Postponed emission of magnetic noise in the $10^{-6} - 5 \times 10^{-1}$ Hz frequency range was observed in stationary conditions in contrast to Barkhausen noise.

DOI: 10.1103/PhysRevB.94.144421

I. INTRODUCTION

Diversity of unusual spin structures or nonlinear spin ensembles was found in chiral molecular magnets, which manifest competition of magnetic anisotropy in sublattices, coexistence of symmetrical and nonsymmetrical exchange interactions, and large lattice parameters comparable with domain wall width. The abovementioned factors provide nonlinear magnetic response of chiral molecular magnets recognized in anomalous temperature dependences of magnetization [1], generation of nonlinear spin excitations by microwave magnetic field [2], bistability of the ferromagnetic resonance [3], and Peierls dynamics of domain walls [4]. In thin helimagnetic films of inorganic materials [MnSi, FeGe, (FeCo)Si], nonlinear ensembles of spins are well known as skyrmions demonstrating sudden restructuration under an applied critical magnetic field [5–7].

In contrast to regular transitions in skyrmion lattices, stochastic magnetization jumps can be observed in most ferromagnetic media as Barkhausen jumps appearing due to the irreversible displacement of domain walls, decay of single domain states, or nucleation of new domains [8]. Though stochastic Barkhausen jumps can be expected in metal-organic molecular magnets, no experimental evidence of domain wall existence as well as observation of stochastic jumps were published, to our knowledge. Additionally to domain wall avalanches, magnetization jumps can appear due to a sudden rearrangement of spin exchange interaction in linear chains [9] or transformation of internal structure of spin solitons [10]. Stochastic magnetization jumps manifested in a sweeping reverse magnetic field were experimentally found in recent papers [11,12]. Direct experimental evidence of the spin-soliton origin of magnetization jumps in a $Cr_{1/3}NbS_2$ chiral helimagnet was reported in Ref. [13]. Experimental observation of magnetization jumps in a $K_{0.4}[Cr(CN)_6][Mn(R/S)\text{-}pn](R/S)\text{-}pnH_{0.6}$ ferrimagnet [11,12] did not allow one to estimate the energy landscape of elementary demagnetization events. Continuous magnetic relaxation in molecular magnets is also an exotic unclear process mentioned in very few articles [14]. Do molecular magnets follow exponential or logarithmic relaxation dynamics? Is it possible to describe a magnetic field and temperature dependences of relaxation by existing models of the domain wall unpinning [15,16]? These questions are still open, and we will create experimental conditions to answer them.

In this paper, we report on the new magnetic phenomenon, which is postponed emission of magnetic noise in the $10^{-6} - 5 \times 10^{-1}$ Hz frequency range. In contrast to ordinary Barkhausen jumps, we observed stochastic magnetization jumps in a stationary magnetic field after it was stabilized down from a saturation field. Metastable spin ensembles relaxing under thermal fluctuations require long expectation time up to $\sim$10 min before they contribute to a spin avalanche. Delayed demagnetization of the sample is provided by a rearrangement of intrinsic structure of large spin ensembles coupled by exchange interaction. The importance of observation of postponed magnetization jumps consists of the contribution of this phenomenon to the list of the fundamental and unusual physical effects associated with nonlinear systems. One of the most famous examples of such nonlinear emission is laser manifesting delayed relaxation of metastable excited atomic states. Similarly to that, magnetization jumps observed in our work in a stationary magnetic field are a spontaneous emission of the events corresponding to relaxation of metastable spin states of nonlinear magnetic ensembles. The origin of postponed magnetization of the jumps is strongly different from well-known Barkhausen jumps because the last ones

*morgunov2005@yandex.ru

require a magnetic field sweep to provide S-shaped instability of the domain wall dynamics. The absence of this condition in our experiments proves a new kind of magnetic instability corresponding to the observed jumps.

We present the analysis of statistical regularities of stepwise demagnetization of a $K_{0.4}[Cr(CN)_6][Mn(R/S)\text{-pn}](R/S)\text{-pn}H_{0.6}$ ferrimagnet in sweeping and stationary magnetic fields as well as search for discrete magnetization and energy levels corresponding to conformations of spin solitons and other spin ensembles. Continuous magnetic relaxation and its comparison with existing models developed for domain wall mechanisms of relaxation are also of interest.

II. EXPERIMENTAL

Chemical synthesis, x-ray analysis, and express attestation of the simplest magnetic properties (coercive field H_{coer} and Curie temperature $T_C = 53$ K) of studied crystals are well known [17]. The needle-shaped single crystal was $1.5 \times 0.5 \times 0.1$ mm^3 in size. The volume of the elementary crystal cell containing Mn^{2+} and Cr^{3+} ions was $V_0 = 3318.75$ Å^3. The total number of spins in volume V of the sample was $N = V/V_0 \approx 2.26 \times 10^{16}$.

The magnetic moment of the sample and its time, field, and temperature dependences were recorded by a MPMS 5XL Quantum Design superconducting quantum interference device (SQUID) magnetometer. All measurements were performed in the 2–50 K temperature range, where the sample was ferrimagnetically ordered excepting the low-temperature range (2–10 K), manifesting spin canted phase due to the Dzyaloshinskii-Moriya interaction [1,18]. The sample was cooled before experiments in zero magnetic field and magnetized in a saturation field. The external magnetic field was directed along the easy magnetization axis. The saturation magnetization at $T = 2$ K in the magnetic field $H \geq 400$ Oe corresponds to the effective magnetic moment $M_{SAT} = 2\,\mu_B$ being in agreement with the antiparallel orientation of Cr^{3+} and Mn^{2+} spins in the crystal unit cell.

III. EXPERIMENTAL RESULTS AND DISCUSSION

Two types of experiments were performed: the sweeping magnetic field varied in the range from +30 to −10 Oe (with negligibly small steps of magnetic field 0.2 Oe); the stationary magnetic field stabilized down from the saturation value $H_{SAT} = 400$ Oe. Examples of magnetic hysteresis loops at 2 and 8 K are presented in Fig. S1 (see Supplemental Material [19]). Time dependences of the magnetic moment $M(t)$ were recorded in the −50 to +30 Oe magnetic field range. A set of time dependences recorded in the same conditions ($T = 2$ K, measurement field $H^* = +10$ Oe) is presented in Fig. S2 (see Supplemental Material [19]).

A. Magnetization jumps in a linearly sweeping reverse field

In a linearly sweeping magnetic field $dH/dt > 0$, magnetization of the sample was continuous, i.e. no magnetization jumps were observed. Demagnetization of the sample in a reverse magnetic field $dH/dt < 0$ was accompanied by stochastic jumps of the magnetic moment [see insertion in Fig. 1(a)]. The presence of magnetization jumps in the reverse magnetic field was reliably reproducible in the 2–50 K temperature range. The decrease of the magnetic field sweeping rate from 0.0125 to 0.00125 Oe/s resulted in the strong increase in jump number. Maximal flow density of the jumps was observed at the minimal possible sweeping rate of 0.00125 Oe/s. Two types of magnetization jumps were observed. The former type described in detail in Ref. [11] appeared at the reproducible threshold magnetic field H_{C1} (Fig. 1(a); also Fig. S1 in the Supplemental Material [19]). As it was mentioned in Ref. [11], the origin of this jump is a commensurate-incommensurate transition in the spin soliton lattice controlled by the competitive Dzyaloshinskii-Moriya and Heisenberg interactions. The experimental data related to these kind of regular jumps (RJs) are not included in this paper. The contribution of these RJs is easily recognized because its amplitude $\Delta M > 2.5 \times 10^{-5}$ emu is much higher in comparison with other jumps, and H_{C1} lies in the narrow field range from +14 to +18 Oe. The RJ contribution to statistics will be discriminated.

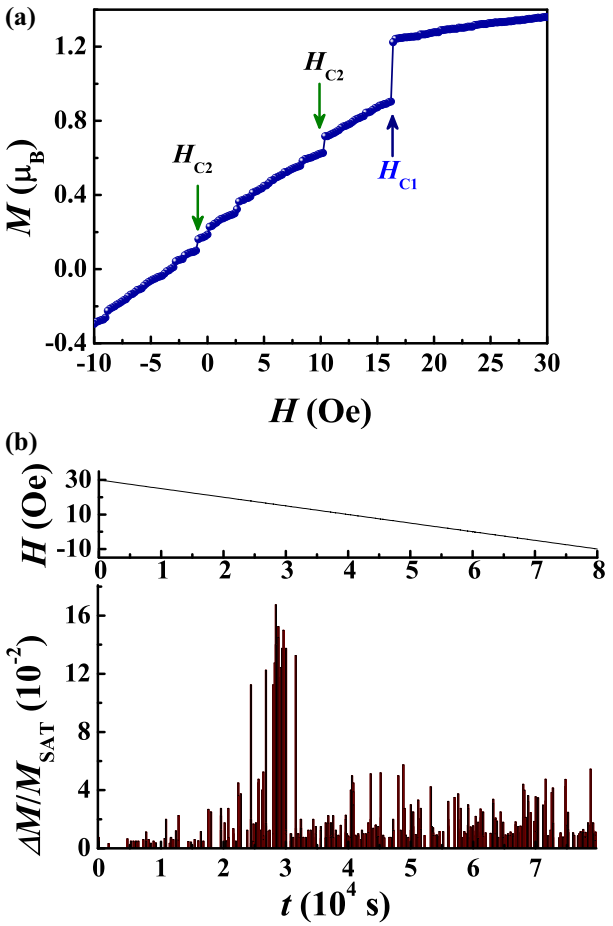

FIG. 1. (a) Dependence of the magnetic moment on the magnetic field $M(H)$ at 8 K. Threshold magnetic fields initiating RJ H_{C1} and SJ H_{C2} are shown by arrows. (b) Superimposed time series of stochastic magnetization jumps collected from 16 independent measurements. Time dependence of magnetic field is presented in the upper panel.

Magnetization jumps of the latter type are irregular stochastic jumps (SJs) whose amplitude is smaller than

2.5×10^{-5} emu. Here, we will focus on the analysis of stochastic jumps of smaller amplitudes. Statistics of these jumps is rich. The minimal amplitude of reliably resolved jumps was $\Delta M = 3 \times 10^{-6}$ emu. The magnetic field at which the SJ appeared H_{C2} was varied in a wide range from +30 to −30 Oe in both direct and reverse magnetic field scanning modes. The correspondent volume of the sample involved in the minimal jump was $V_J = 6 \times 10^{17}$ Å^3 $= 2 \times 10^{14}\, V_0$ (V_0 is volume of the elementary crystal cell). Thus, 1% of atoms are involved in minimal SJ.

A series of independent experiments including 16 reverse field dependences was recorded in the same conditions to obtain a statistical distribution of SJs and regularities of their appearance. An example of 16 superimposed $\Delta M(t)$ dependences is presented in Fig. 1(b). The autocorrelation coefficient of SJ $R_A < 0.1$ was small independently on correlation lag. The correlation coefficient of jump amplitude ΔM and magnetic field H_{C2} was $R_{\Delta MH} < 0.1$. The values of R_A and $R_{\Delta MH}$ indicate the absence of correlations and support the stochastic origin of SJs.

The main parameters of the jumps (normalized amplitude $\Delta M/M_{SAT}$ and magnetic field H_{C2}) were independent on neither previous cycle of experiments nor each other, i.e. the jumps were stochastic. Statistical analysis of the jump distribution in normalized amplitude $\Delta M/M_{SAT}$ and field H_{C2} [Fig. 2(a)] reveals a regularity of jump appearance. All magnetization jumps can be grouped in accordance with the few most probable M_i values between which the jumps occur. Few modes of magnetization jumps correspond to discrete ΔM_i values.

The power spectral density of magnetization SJs $S(f)$ [Fig. 2(b)] was determined by the following algorithm:

(1) Measurements of a set of identical $M(t)$ dependences in the same conditions and accumulation of data array large enough to allow statistical regularities of jump amplitudes ΔM and time correlations to be analyzed.

(2) Selection of a series of magnetization jumps $(t_i, \Delta M_i)$ for each $M(t)$ dependence (t_i is current time of the ith jump, ΔM_i is the ith jump amplitude).

(3) Association of the obtained time series.

(4) Partition of the time scale into N intervals Δt, including no more than one magnetization jump. This partition results in a uniform time series $(t_n, \Delta M_n)$, $n = 1$. N is time interval number, $t_n = n \times \Delta t$, ΔM_n is the amplitude of the magnetization jump occurring during time interval $(t_n - \Delta t/2;\ t_n + \Delta t/2;\ \Delta M_n = 0$ if no jumps occur in the correspondent time interval).

(5) Calculation of the linear autocorrelation coefficient $r(\Delta M_n; \Delta M_{n-k})$ for all allowable lag values $k = 1$. N and determination of $r(k)$ dependence [correlogram of $(t_n, \Delta M_n)$ series] by the formula

$$r(\Delta M_n, \Delta M_{n-k}) = \frac{\overline{\Delta M_n \cdot \Delta M_{n-k}} - \overline{\Delta M_n} \cdot \overline{\Delta M_{n-k}}}{\sigma(\Delta M_n) \cdot \sigma(\Delta M_{n-k})}.$$

Here,

$$\sigma(\Delta M_n) = \sqrt{\frac{1}{N-k}\sum_{n=1+k}^{N} \Delta M_n^2 - \left(\sum_{n=1+k}^{N} \Delta M_n\right)^2}$$

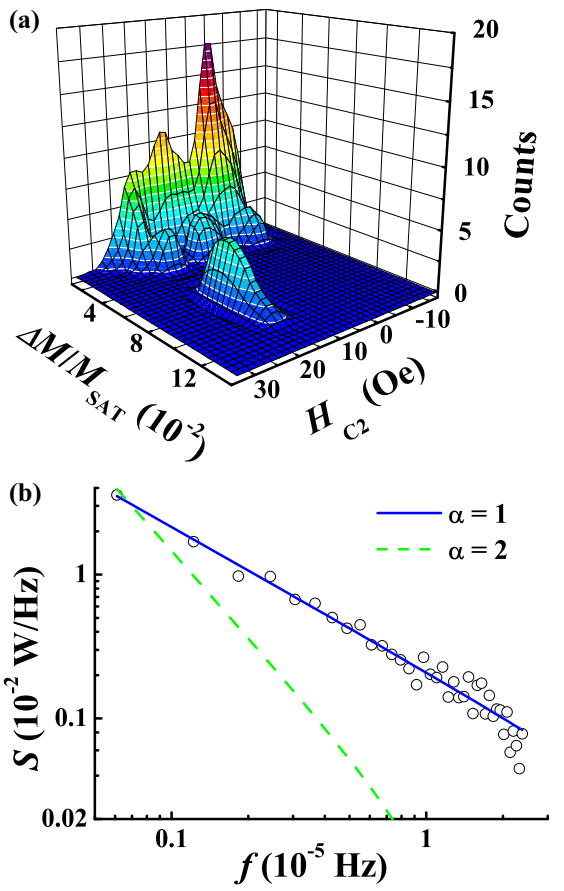

FIG. 2. (a) Distribution of amplitude ΔM and magnetic field H_{C2} of the stochastic magnetization jumps at 8 K in sweeping magnetic field. (b) Spectral density $S(f)$ of the magnetization SJs in a sweeping magnetic field and its approximations by $(1/f)^\alpha$ function (theoretical curves for $\alpha = 1$ and $\alpha = 2$ are shown by dashed and solid lines, respectively).

and

$$\sigma(\Delta M_{n-k}) = \sqrt{\frac{1}{N-k}\sum_{n=1+k}^{N} \Delta M_{n-k}^2 - \left(\sum_{n=1+k}^{N} \Delta M_{n-k}\right)^2}$$

are standard deviations of jump amplitudes, and

$$\overline{\Delta M_n} = \sum_{n=1+k}^{N} \Delta M_n, \quad \overline{\Delta M_{n-k}} = \sum_{n=1}^{N-k} \Delta M_n,$$

and

$$\overline{\Delta M_n \cdot \Delta M_{n-k}} = \frac{1}{N-k}\sum_{n=1+k}^{N} \Delta M_n \cdot \Delta M_{n-k}$$

are sample means in samples involved in comparison to obtain $r(\Delta M_n; \Delta M_{n-k})$.

(6) Accordingly, with the Wiener-Khinchin theorem [20], the spectral density of noise power $S(f)$ can be evaluated from correlogram $r(k)$ by the discrete Fourier transform

$$S(f_n) = \sum_{k=1}^{N} r(k) \cdot e^{-(2\pi i/N)k f_n \Delta t}, \qquad (1)$$

where $f_n = \frac{n}{N\Delta t}$, $n = 1$. N is output frequency set of the discrete Fourier transform.

This algorithm is used because the set of events $(\Delta M_k; t_k)$ is discrete. If the set of events $\Delta M(t)$ is continuous and the Fourier transform of $\Delta M(t)$ exists, spectral power $S(f)$ can be found from $\Delta M(t)$ directly

$$S(f) = \frac{1}{T}\varphi(f)\cdot\varphi^*(f) = \frac{1}{T}|\varphi(f)|^2,$$
$$\varphi(f) = \int_0^T \Delta M(t)e^{-2\pi i f t}dt,$$

where $\varphi(f)$ is the Fourier transform of the signal, and T is recording time. The spectral density of SJs in our experiments is presented in Fig. 2(b).

The frequency range f corresponds with periods exceeding the scanning time of the magnetic field. The approximation of the spectral density by $(1/f)^\alpha$ function resulted in the best fitting at $\alpha = 1 \pm 0.1$. The value $\alpha = 1$ corresponds with $1/f$ pink noise [21]. This kind of noise is a fingerprint of self-organized criticality indicating multiscale parallel relaxation processes. The corresponding fractal organization of the relaxation processes is evidence of interaction between relaxing spin ensembles and the scale-invariant character of the studied events [21].

B. Postponed magnetization jumps in stationary reverse magnetic field

In this section, relaxation of the magnetic moment [time dependences $M(t)$] was recorded in a stationary magnetic field H varied in the range from -50 to $+30$ Oe. The experimental consequence is shown in Fig. S3 (see Supplemental Material [19]). On the background of continuous relaxation (the series of the selected jump-free $M(t)$ curves is shown in Fig. S4; see Supplemental Material [19]), a series of sharp jumps of the magnetic moment is clearly distinguishable in the 9–10.5 Oe field range [Fig. 3(a)]. The jump amplitude ΔM was determined as a difference between magnetic moments corresponding to initial and final zero values of the dM/dt derivative [insertion in Fig. 3(a)]. A series of 20 measurements of the same sample in the same conditions (temperature, magnetic field, duration of measurements, etc.) was performed to accumulate the data bank large enough for statistical treatment (Fig. S2; see Supplemental Material [19]). A superimposition of 20 time dependences is presented in Fig. 3(b). The distribution of the jump amplitude ΔM and time t_C passed after stabilization of the switched magnetic field H is presented in Fig. 4(a). One can distinguish discrete starting magnetization levels M_i and a few discrete values of the magnetization jumps ΔM_i corresponding with energy levels of the spin system E_i numerated by integer value i [Fig. 4(b)]. The changes in the Zeeman energy of the spin ensemble accompanying the transition from energy level E_1 to energy E_i is $\Delta E_n = (\Delta M_i - \Delta M_1) \times H_C$, where $i = n + 1$, n is number of transitions. Thus, unimodal, bimodal, and three-modal distributions of the magnetization jump amplitude were found in the studied crystals. Each mode corresponds to discrete change in energy of the spin ensemble ΔE_n, manifesting a discrete energy spectrum of the system. Observed jumpwise relaxation is not Barkhausen noise because the latter is a response of the system to a rapidly sweeping magnetic field. The autocorrelation coefficient of SJs in stationary conditions was weak ($R_A = 0.1$) as well as the correlation coefficient between the jump amplitude ΔM and expectation time t_C($R_{\Delta M-tc} < 0.1$). The Fourier transform described by the formulas in Eq. (1) results in frequency-independent spectral density, i.e. $1/f^\alpha$, $\alpha = 0 \pm 0.1$ [Fig. 4(c)]. This kind of stochastic event is known as white noise [21]. Thus, we observed a unique switch of pink to white noise by changing experimental conditions from a sweeping to a stationary magnetic field.

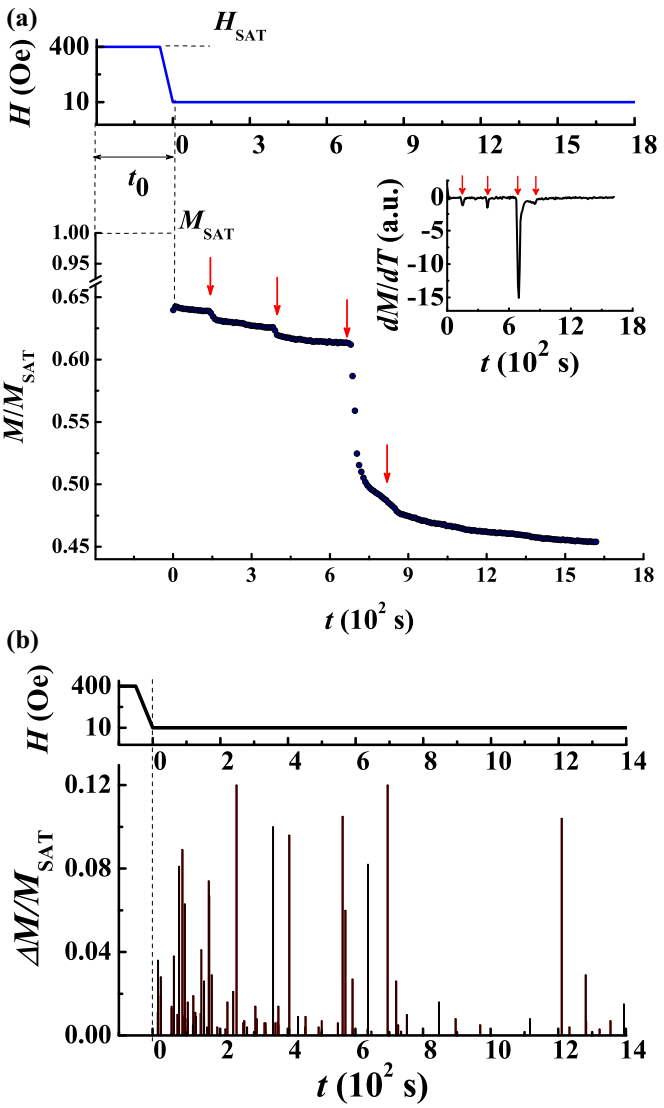

FIG. 3. (a) Time dependence of the magnetic moment $M(t)$ recorded after a magnetic field +10 Oe was stabilized at $T = 2$ K. In the insertion, the derivative $dM(t)/dt$ is presented. Arrows indicate magnetization jumps. (b) Superimposed time series of stochastic magnetization jumps collected from 20 independent measurements. Time dependence of magnetic field is presented in the upper panel.

The power spectra of white, pink, and brown noise suggest the generalization [22–26] towards power-law functions $S(f)$ with arbitrary exponents. Fractional Brownian motion (FBM) is a statistical process where both real and imaginary parts of the Fourier amplitudes $\varphi(f)$ are Gaussian-distributed random

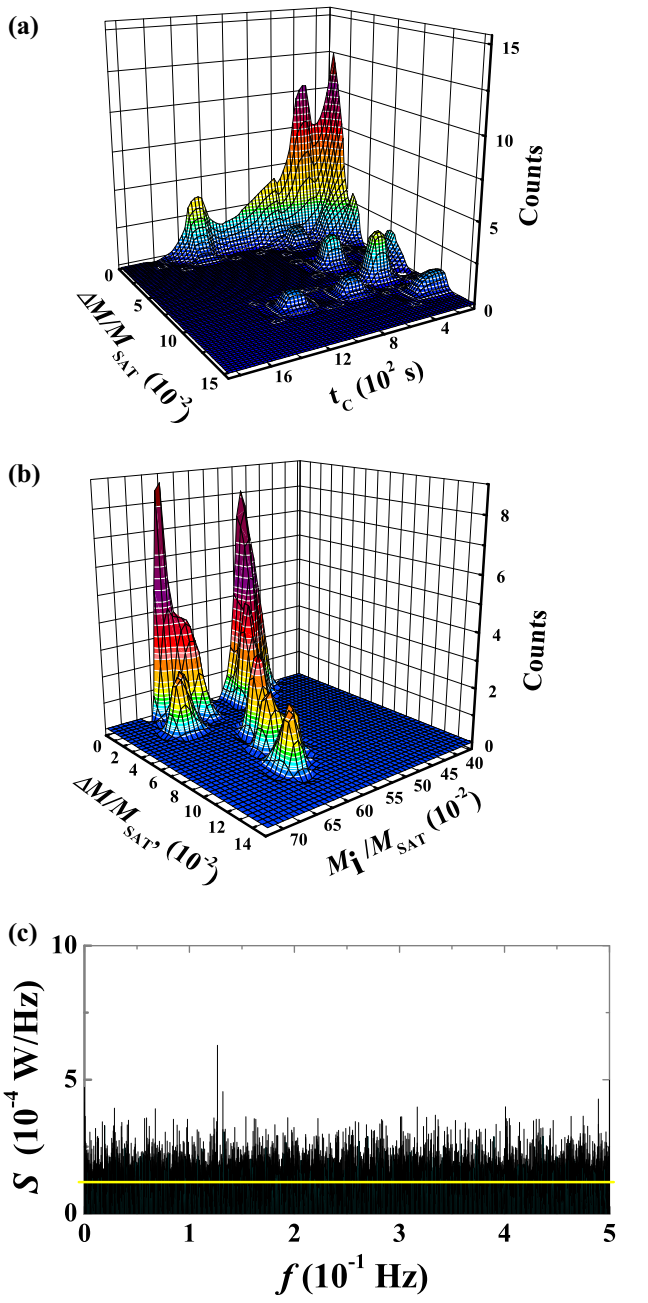

FIG. 4. (a) Distribution of amplitude ΔM and expectation time t_C of the magnetization SJs in stationary magnetic field at 2 K. (b) Distribution of amplitude ΔM and starting magnetic moment M_i of the magnetization SJs in stationary magnetic field at 2 K. (c) Spectral density $S(f)$ of the magnetization SJs in stationary magnetic field. Expected value is shown by horizontal solid line.

variables with $\overline{\varphi(f)} = 0$ and $\overline{\varphi(f)\phi(f')^*} = S(f)\delta(f - f')$ with $S(f) \propto |f|^{-\beta}$.

Exponent β is called spectral exponent of the process. White, pink, and brown noises are FBMs with $\beta = 0$, 1, and 2, respectively. The term FBM can be motivated from its relationship to fractional derivatives or fractional integration. Generally, deriving function $\Delta M(t)$ in time corresponds to multiplying its Fourier amplitudes $\varphi(f)$ by $2\pi if$ [26]. The

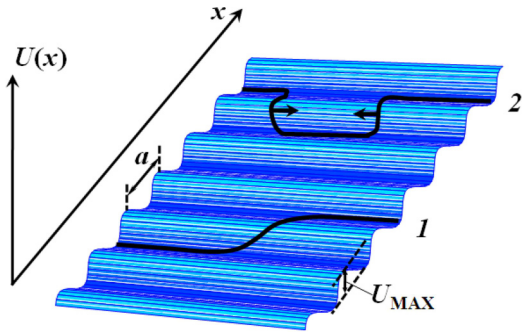

FIG. 5. Sketch of (1) single kink and (2) double kink formed on the domain walls in periodical potential relief of crystal lattice (a is lattice parameter), U is potential energy of amplitude U_{MAX}. Self-contraction forces are shown by arrows.

fraction derivative can be defined as

$$\frac{\partial^\alpha}{\partial t^\alpha}\Delta M(t) = \int_{-\infty}^{\infty} \varphi(f)(2\pi if)^\alpha e^{2\pi ift} df$$

for arbitrary real numbers α. This definition as applied to negative values of α leads to fractional integration. In this sense, FBM with spectral exponent β arises from applying fractional integration with $|\alpha| = \beta/2$ to white noise. Thus, in terms of fractional derivatives, pink noise ($\beta = 1$) arises from applying half of a derivative to Brownian motion ($\beta = 2$) or half of integration to white noise ($\beta = 0$).

Since pink noise results from fractional integration of white noise, one can conclude that a sweeping magnetic field provides fractional integration of the noise appearing in stationary conditions. The changes in the noise spectra under a sweeping magnetic field are obvious. In our previous publication [4], an important feature of the studied molecular ferrimagnets was analyzed. The balance between exchange interaction and magnetic anisotropy provides comparatively narrow domain walls, which width W is ~3–4 a (a is the crystal lattice parameter). In accordance with the classical models of domain wall dynamics [27], narrowness of the domain walls results in unusual nonlinear dynamics similar to dislocation kink dynamics in deformed solids [28]. Periodical potential relief (Peierls relief) strongly contributes to the formation of solitonlike spin ensembles along a domain wall [28]. The formation of single and double kinks along the domain wall (Fig. 5) can be described by the sine-Gordon equation [28]. In the presence of an external magnetic field, the formation of kinks is a thermoactivated process similar to that in dislocation theory. The activation energy of kink nucleation is comparable with the height of the Peierls relief U_{MAX}. In the absence of an external magnetic field or in a diminished field, kink annihilates under self-interacting forces (Fig. 5). Kink annihilation as well as its nucleation is a thermoactivated process. Random potential of structural defects results in kink pinning and can be overcome during expectation of thermal fluctuation. The activation energy of this process E_a controlled by structural defects is generally different from U_{MAX}. Each observed magnetization jump includes contributions of many kinks, which nucleation and annihilation can be correlated by interkink magnetic interactions. Indirect evidence of the proposed description is a nonmonotonous temperature

dependence of critical magnetic field of the magnetization jump [11]. This nonmonotonous behavior possibly originates from the competition between annihilation and nucleation of the kinks.

One can suppose that postponed magnetization jumps can be observed in the class of materials satisfying the condition $W \sim a$. This class of ferromagnets includes strong rare-earth magnets RE-TM-B [29], yttrium garnet films [30], and other materials, in which exchange interaction and magnetic anisotropy result in narrow domain walls. In the materials, where domain walls are wide, the Peierls relief does not contribute to domain wall mobility. In that case, a sharp decrease of the external magnetic field (in particular, the decrease down to zero field) does not result in postponed magnetization jumps because there are no driving forces in the absence of kinks (self-interaction of kinks is absent).

The above-discussed interpretation is in agreement with the experimentally observed difference between colors of magnetic noise in a sweeping magnetic field (pink noise, see Sec. III.A) and a stationary magnetic field (white noise, Sec. III.B). Magnetic field sweeping causes nucleation of kinks possessing self-organizing criticality, i.e. multiplication of elementary events resulting in pink noise takes place. In the stationary magnetic field, spontaneous independent annihilations of the kinks dominate. In that case, there are no self-organized processes. White noise indicates the absence of self-organization.

Obviously, Fig. 5 is a simplified conditional image of the Peierls relief. Real crystal structure and spin ordering in studied crystals are more complicated. The Dzyaloshinskii-Moriya interaction produces helicity of spin magnetic structure in the studied crystals accompanied with vortex Hubert domain walls [31]. Nevertheless, we believe in the correctness of the above-described mechanism of postponed magnetization jumps because vortex domain walls are sensitive to periodical lattice potential [31].

C. Continuous component of magnetic relaxation

Finally, we will discuss the continuous component of relaxation of the magnetic moment. For that purpose, jump-free $M(t)$ curves were recorded in +50 to −30 Oe fields (Fig. 6; also see Fig. S4 in the Supplemental Material [19]). Continuous relaxation occurs in positive (Fig. 6, curve 1) and negative fields H^* (Fig. 6, curves 2, 3), both. The slope of the relaxation curve increases as H^* approaches coercive field H_{coer}. Magnetic relaxation provided by dynamics of the domain walls can be studied successfully by analyzing time dependences of magnetization. Most of the ferromagnetic materials manifest logarithmic dependences of the magnetic moment $M(t)$ in a reverse magnetic field [32,33]

$$M = M_0 - S \cdot \ln(t - t_{01}), \tag{2}$$

where S is magnetic viscosity, t_{01} is time of reverse field stabilization, M_0 is the initial magnetic moment stabilized after magnetic field fixation. Magnetic viscosity characterizes activation energy of the process responsible for magnetic moment relaxation. The distribution of relaxation times $f(\tau)$ can be derived from the temperature and field dependences of

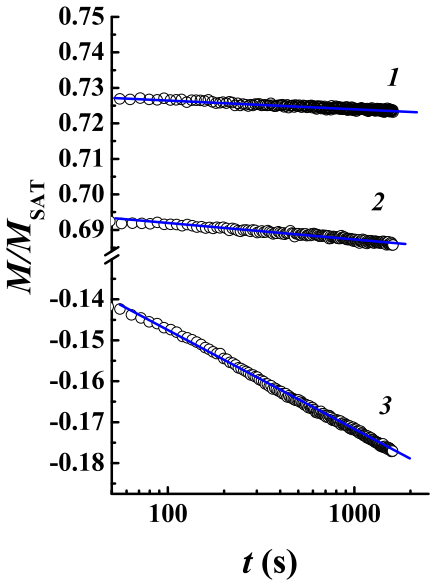

FIG. 6. Jump-free fragments of continuous magnetic relaxation in stationary magnetic field (1) 30 Oe, (2) 20 Oe, and (3) −18 Oe at $T = 2$ K. Approximations by the formula in Eq. (2) are shown by solid lines. The sample was magnetized in saturating magnetic field $H_{SAT} = 400$ Oe during the 5 min before experiments.

magnetic moment due to the following equation [32,33]:

$$M(t) = \int_0^{\tau_1} M_0 \exp\left(-\frac{t}{\tau}\right) f(\tau)\, d\tau.$$

Straightening of the $M(t)$ dependences in semilogarithmic coordinates (Fig. 6) indicates the validity of the formula in Eq. (2) and the equiprobable distribution of potential demagnetization barriers among their relaxation time τ and correspondent height [32,33]. The approximation of the $M(t)$ dependences recorded in reverse magnetic field H^* by the formula in Eq. (2) (Fig. 6), allows us to determine S values at different temperatures. Instead of S, we used normalized viscosity S_V since it is independent on demagnetization factors and sample shape $S_V = S/\chi_{irr}$, where χ_{irr} is irreversible magnetic susceptibility determined by the equation $\chi_{irr} = \chi/(1 + N\chi)$ [15,16,32,33], $\chi = dM/dH$ is the tangent slope for the demagnetization part of the hysteresis loop and $N \approx 0$ is the demagnetizing factor of the needle-shaped sample. The temperature dependence of normalized magnetic viscosity $S_V(T)$ is presented in Fig. 7. In the $T = 2 - 20$ K temperature range, the S_V value decreases, while at $T > 20$ K the S_V value increases. The linear temperature dependence of magnetic viscosity agrees well with the theory of domain wall pinning [15,16,32,33], allowing us to estimate activation volume V^* of the obstacle overcome by a domain wall

$$S_V = k_B T/(V^* M_{SAT}), \tag{3}$$

where k_B is the Boltzmann constant. In the 20–50 K temperature range, the dependence $S_V(T)$ can be considered as a linear one in agreement with the prediction by the formula in Eq. (3) (top x and right y axes in Fig. 7). The approximation of this dependence by the formula in Eq. (3) results in activation volume $V^* = 4.4 \times 10^{10}$ Å^3 $= 10^7\, V_0$.

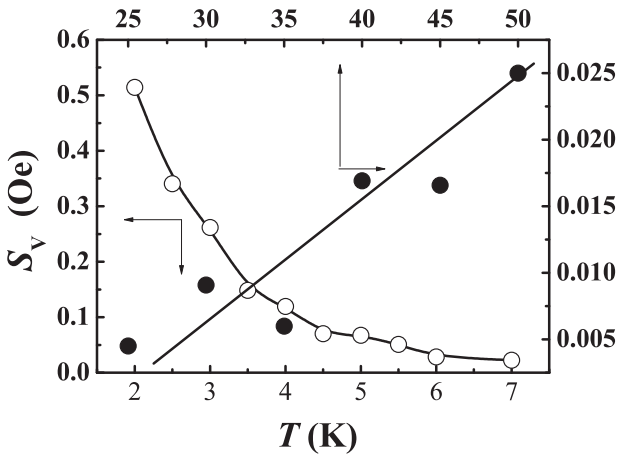

FIG. 7. Temperature dependence of normalized magnetic viscosity S_V in reverse magnetic field $H = -H_{coer}$. Approximation of the high-temperature part of the S_V (T) dependence by the formula in Eq. (3) is shown by solid line.

This parameter is a few orders of magnitude higher than the volume corresponding with the turn of a single 180° domain wall caused by remagnetization: $V_1^* = \delta^3 = 1.98 \times 10^6$ Å^3 $\sim 10^3\, V_0 (\delta = \pi(A/K)^{1/2}$ is domain wall thickness [4] determined by exchange constant $A = 1.6 \times 10^{-8}$ erg/cm and $K = 10^5$ erg/cm anisotropy constant). However, V^* is smaller than the volume involved in the magnetization jump $V_J = 6 \times 10^{17}$ Å^3 $= 2 \times 10^{14}\, V_0$. Thus, the estimation resulted from thermoactivation analysis gives an intermediate value: $V_1^* \ll V^* \ll V_J$. This volume corresponds to the ensemble of domain walls simultaneously contributing to continuous relaxation.

The estimated activation volume expressed in δ^3 units $V^* \sim 10^4\, \delta^3$ exceeds typical values in inorganic magnets, where $V^* \sim 10\delta^3$ [34]. This difference appears due to the large size of the elementary cell in molecular magnets and exceeds the typical value of this parameter in inorganic materials up to ~10 times. At $T < 10$ K, cooling causes a sharp increase of the S_V value (Fig. 7) that is in contradiction with the classical theory of domain wall motion. The possible explanation of this phenomenon is a rearrangement of the intrinsic spin structure of large spin ensembles responsible for the observed jumps. One can suppose that the same spin ensembles, whose contribution to the stepwise relaxation was observed by us at low temperatures, can also contribute to continuous demagnetization unresolved by slow SQUID technique. In that case, one can perceive the continuous part of the $M(t)$ dependence as an envelope of small demagnetization jumps.

IV. CONCLUSION

Postponed jumpwise relaxation of the magnetic moment in a stationary magnetic field was found in a $K_{0.4}[Cr(CN)_6][Mn(R/S)\text{-}pn](R/S)\text{-}pnH_{0.6}$ molecular ferrimagnet. Statistical analysis of magnetization jumps (their amplitude and time) revealed discrete magnetization levels and corresponding energy spectra of the nonlinear spin ensembles. The discrete energy spectrum characterizes the intrinsic structure of the unknown spin ensemble, whose structure is different from that of standard domain walls and skyrmions. White noise corresponding with relaxation of the spin ensembles in a stationary magnetic field can be turned to pink noise in a sweeping magnetic field. A continuous part of magnetic relaxation indicates the presence of new spin ensembles at low temperatures (2–10 K). Magnetic viscosity determined from the analysis of the flowing part of the magnetic relaxation corresponds to avalanches of domain walls at high temperatures (20–50 K). The obtained results seem to be important for discussion of new nonlinear spin ensembles (solitons) early reported in numerous articles [1,10–12,17,18] and references therein. In general, the significance of the results relates to the physics of nonlinear phenomena, where magnetic excitations (spin waves, solitons, breathers, skyrmions, etc.) can be considered as modeling situations reproducible in laboratory conditions. At the same time, the conclusion can be extended to other areas where periodicity of space potential contributes to the formation of nonlinear excitations. Another possible contribution of the obtained results consists of realization of fractional integration transforming white noise to pink noise under the action of a sweeping magnetic field.

ACKNOWLEDGMENTS

The paper was supported by the Russian Foundation for Basic Research Project No. 15-02-05149 a.

[1] J. Kishine, K. Inoue, and Y. Yoshida, Prog. Theor. Phys. Suppl. **159**, 82 (2005).
[2] R. B. Morgunov, M. V. Kirman, K. Inoue, Y. Tanimoto, J. Kishine, A. S. Ovchinnikov, and O. Kazakova, Phys. Rev. B **77**, 184419 (2008).
[3] R. B. Morgunov, F. B. Mushenok, and O. Kazakova, Phys. Rev. B **82**, 134439 (2010).
[4] F. Mushenok, O. Koplak, and R. Morgunov, Eur. Phys. J. B **84**, 219 (2011) .
[5] A. B. Butenko, A. A. Leonov, U. K. Rößler, and A. N. Bogdanov, Phys. Rev. B **82**, 052403 (2010).
[6] A. Karhu, U. K. Rößler, A. N. Bogdanov, S. Kahwaji, B. J. Kirby, H. Fritzsche, M. D. Robertson, C. F. Majkrzak, and T. L. Monchesky, Phys. Rev. B **85**, 094429 (2012).
[7] M. N. Wilson, E. A. Karhu, D. P. Lake, A. S. Quigley, S. Meynell, A. N. Bogdanov, H. Fritzsche, U. K. Rößler, and T. L. Monchesky, Phys. Rev. B **88**, 214420 (2013).
[8] G. Catalan, J. Seidel, R. Ramesh, and J. F. Scott, Rev. Mod. Phys. **84**, 119 (2012).
[9] A. S. Boyarchenkov, I. G. Bostrem, and A. S. Ovchinnikov, Phys. Rev. B. **76**, 224410 (2007).

[10] J. Kishine, I. G. Bostrem, A. S. Ovchinnikov, and Vl. E. Sinitsyn, Phys. Rev. B **89**, 014419 (2014).
[11] A. D. Talantsev, M. V. Kirman, and R. B. Morgunov, Phys. Status Solidi B **253**, 1222 (2016) .
[12] M. V. Kirman, A. D. Talantsev, O. V. Koplak, and R. B. Morgunov, JETP Lett. **101**, 398 (2015).
[13] K. Tsuruta, M. Mito, Y. Kousaka, J. Akimitsu, J. Kishine, Y. Togawa, H. Ohsumi, and K. Inoue, J. Phys. Soc. Jap. **85**, 013707 (2016).
[14] M. Sendek, K. Csach, V. Kavečanský, M. Lukáčová, M. Maryško, Z. Mitróová, and A. Zentko, Phys. Status Solidi A **196**, 225 (2003).
[15] D. Givord, Q. Lu, M. F. Rossignol, P. Tenaud, and T. Viadieu, JMMM **83**, 183 (1990).
[16] C. K. Mylvaganam and P. Gaunt, Philos. Mag. B **44**, 581 (1981).
[17] K. Inoue, H. Imai, P. S. Ghalsasi, K. Kikuchi, M. Ohba, H. Okawa, and J. V. Yakhmi, Angew. Chem. Int. Ed. **40**, 4242 (2001).
[18] J. Kishine, K. Inoue, and K. Kikuchi, JMMM **310**, 1386 (2007).
[19] See Supplemental Material at http://link.aps.org/supplemental/10.1103/PhysRevB.94.144421 for magnetic hysteresis curves and additional data for time dependences of magnetization.
[20] G. M. Jenkins and D. G. Watts, *Spectral Analysis and Its Applications* (Holden-Day, San Francisco, 1968).
[21] H. D. I. Abarbane, R. Brown, J. J. Sidorowich, and L. Sh. Tsimring, Rev. Mod. Phys. **65**, 1331 (1993).
[22] L. Pietronero, *Fractals' Physical Origin and Properties* (Springer, New York, 1989), p. 68.
[23] B. B. Mandelbrot and J. W. Van Ness, SIAM Rev. **10**, 422 (1968).
[24] N. J. Usdin, Proc. IEEE **83**, 802 (1995).
[25] P. Häunggi and P. Jung, Adv. Chem. Phys. **89**, 239 (2007).
[26] S. Hergarten, *Self-Organized Criticality in Earth Systems* (Springer Science and Business Media, New York, 2013), p. 49.
[27] H.-R. Hilzinger and H. Kronmuller, Phys. Lett. A **51**, 59 (1975).
[28] F. J. Buijnsters, A. Fasolino, and M. I. Katsnelson, Phys. Rev. Lett. **113**, 217202 (2014).
[29] J. F. Herbst, Rev. Mod. Phys. **63**, 819 (1991).
[30] K. S. Novoselov, A. K. Geim, S. V. Dubonos, E. W. Hill, and I. V. Grigorieva, Nature **426**, 812 (2003).
[31] F. Li, T. Nattermann, and V. L. Pokrovsky, Phys. Rev. Lett. **108**, 107203 (2012).
[32] D. K. Lottis, E. D. Dahlberg, J. A. Christner, J. I. Lee, R. L. Peterson, and R. M. White, J. Appl. Phys. **63**, 2920 (1988).
[33] R. Skomski and V. Christoph, Phys. Status Solidi B **156**, K149 (1989).
[34] P. Gaunt, J. Appl. Phys. **59**, 4129 (1986).